

## 高速原子間力顕微鏡によるカルサイト溶解過程の原子分解能観察

## Atomic-Resolution Imaging of Calcite Dissolution Processes by High-Speed Atomic Force Microscopy

\*福間 剛士<sup>1</sup>\*Takeshi Fukuma<sup>1</sup>

1. 金沢大学

1. Kanazawa University

炭酸カルシウム鉱物は、地球規模の炭素循環において重要な役割を果たし、それにより地球の大気・水質・地質環境に大きな影響を及ぼす。なかでもカルサイトは、最も豊富に存在し、かつ、反応性に富むため、その結晶成長・溶解過程はとりわけ重要である。特に、最近では大気中の二酸化炭素濃度の上昇を抑制するために、地中への大規模かつ長期的な炭素貯蔵が検討されており、貯蔵された炭素の漏洩の原因となるカルサイトの結晶溶解過程は、大きな注目を集めている。このような長期的かつ大規模な炭素循環を正確に予測するためにも、カルサイト結晶の溶解機構を正確に知る必要がある。

これまでにも、カルサイトの溶解過程は様々な手法により研究されてきた。マクロな挙動については、溶解過程に伴う溶液中のイオン濃度変化を解析することで研究が進められてきた。ナノスケールの挙動については、原子間力顕微鏡 (AFM) や光学的な手法により、単原子ステップのフローを実空間観察することで、その溶解機構が研究されてきた。しかし、原子レベルの結晶溶解モデルを理解するためには、ステップ近傍の原子レベルの挙動を正確に知る必要がある。しかし、従来の分析手法ではこれを直接観察することが困難であったため、未確立の部分が残されている。

周波数変調原子間力顕微鏡 (FM-AFM) は従来超高真空中での原子・分子レベルの表面構造・物性計測に用いられてきた技術である。2005年に我々は、この顕微鏡を液中で動作させる技術を開発し、液中原子分解能観察を可能とした。さらに、近年、我々は液中FM-AFMの観察速度を、従来の~1 frame/minから~1 frame/secへと格段に向上させることに成功した。本研究では、この高速FM-AFMを用いて、カルサイトの溶解過程を直接原子分解能観察することに成功した。その結果、溶解途中の単原子ステップ近傍に、1-8 nm程度の幅を持つ遷移領域が存在することを発見した。この遷移領域の起源については、現在検討段階であるが、原子レベルの結晶溶解機構の理解を大きく進める発見であることは間違いない。このように、従来見ることのできなかつリアルタイムの構造変化を直接観察する技術により、今後、様々な結晶の成長・溶解過程に関する理解が進むものと期待される。

キーワード：原子間力顕微鏡、カルサイト、結晶溶解

Keywords: Atomic Force Microscopy, Calcite, Crystal Dissolution

固液界面の原子スケール観察によるモンモリロナイトのイオン交換に対する水和構造依存性の解明  
Dependence of ion exchange on the hydration structure of montmorillonite surfaces probed  
by atomic-scale observation of solid-liquid interface

\*荒木 優希<sup>1</sup>、佐藤 久夫<sup>2</sup>、大西 洋<sup>1</sup>

\*Yuki Araki<sup>1</sup>, Hisao Satoh<sup>2</sup>, Hiroshi Onishi<sup>1</sup>

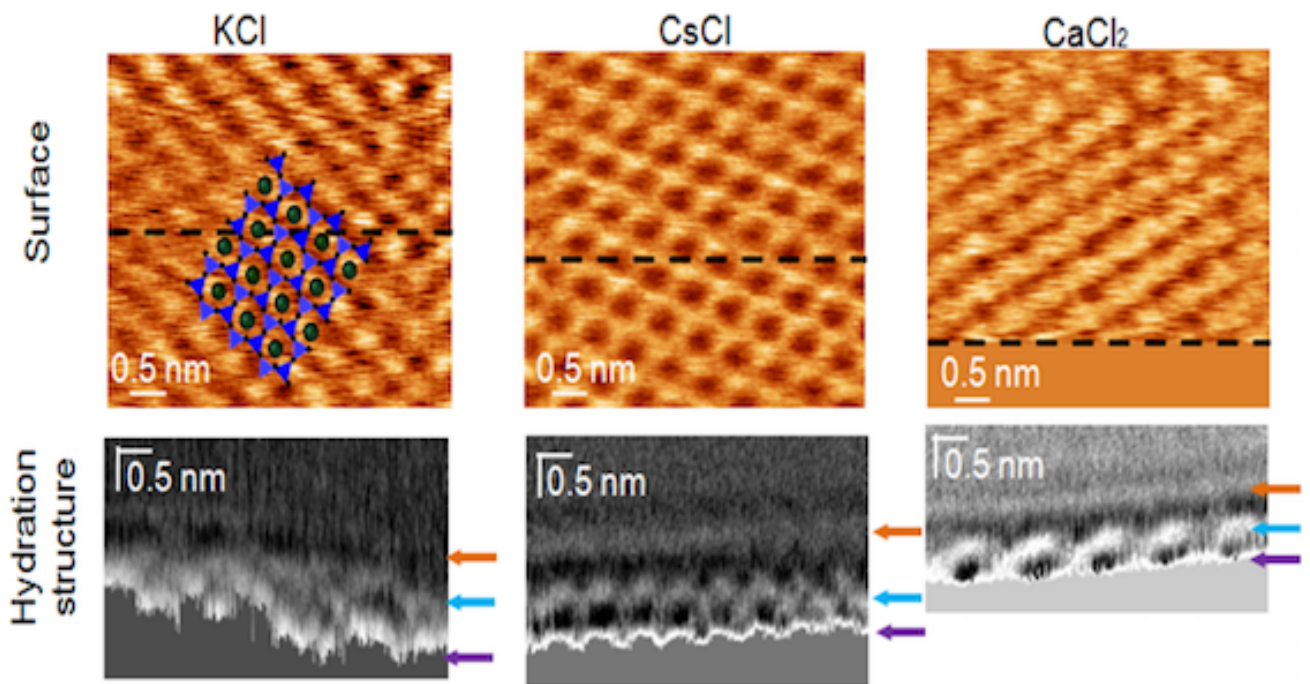
1.神戸大学大学院理学研究科、2.三菱マテリアル

1.Graduate School of Science, Kobe University, 2.Mitsubishi Materials Corporation

Cations of clay mineral are exchangeable depending on the atomic weight and electric density. Because of this ion exchange property, the clays are expected to capture the radionuclide which is diffused in the soil. Recently, the effect of water molecules on the ion exchange tendency has been suggested (S. Charles et al., 2006). In order to clarify the behavior of the water molecules at the clay-solution interface, we conducted the atomic-scale observation of the hydration structure in the vicinity of the montmorillonite surfaces in several ionic solutions. The frequency modulation atomic force microscopy (FM-AFM) which was modified based on the commercial AFM (SPM-9600, Shimadzu Corp., Japan) was employed for the atomic scale observation of interfacial structure (T. Fukuma et al., 2005). This FM-AFM technique has achieved the visualization of the 2D or 3D density map of the water molecules in the vicinity of crystal surfaces (K. Kimura et al., 2010; T. Fukuma et al., 2010). We observed the natural montmorillonite surfaces by FM-AFM in the 0.1 M KCl, CsCl, CaCl<sub>2</sub> solutions, respectively. The 100 nm plate-like particles of the montmorillonite were fixed on the mica substrate surfaces, then the (001) face and the interface were observed (Fig.1). The upper images in Fig.1 show the topography of the montmorillonite surfaces. The protrusions (brighter areas) indicate the cation sites of the montmorillonite surfaces which were located in the center of the six-membered rings of silicate tetrahedra. The interface of the montmorillonite and the solutions were observed along the dashed line in the upper images (bottom images in Fig.1). The bottom images showed the three brighter layers presented by arrows. These brighter areas indicate the distribution of the hydrated water molecules. Our results revealed that the hydration structure in the vicinity of the montmorillonite surfaces is uniform regardless of the cations in the solutions. It is suggested that the water molecules around the surface would not affect the ion exchange at the clay surfaces.

キーワード：粘土鉱物、イオン交換、水和、周波数変調方式原子間力顕微鏡

Keywords: clay mineral, ion exchange, hydration, frequency modulation AFM (FM-AFM)



Electron Backscatter Diffraction (EBSD)法による結晶方位同定のためのEuler角の検討  
Euler angle calculation and evaluation for orientation indexing of Electron Backscatter  
Diffraction(EBSD)

\*森田 博文<sup>1</sup>、Goulden Jenny<sup>2</sup>

\*hirobumi morita<sup>1</sup>, Jenny Goulden<sup>2</sup>

1. オックスフォードインストゥルメンツ株式会社、2. Oxford Instruments Nanoanalysis

1. Oxford Instruments KK, 2. Oxford Instruments Nanoanalysis

近年走査型電子顕微鏡(SEM)を用いた電子線散乱回折(Electron Backscatter Diffraction)－いわゆるSEM-EBSD法の地質学領域への応用が広がっているが、これまでの金属学の領域での応用の多くは立方晶での方位解析であった。しかし次第に金属・半導体・地質などのより広い領域や複雑な材料に広がるにつれて、六方晶や正方晶などの180度対称性の結晶への応用の必要性が高まってきている。EBSD法では菊池パターンから指数付けを行っているので、菊池パターンの対称性で識別できない方位に関しては方位を完全に決定することは難しい場合がある。さらに測定試料を70度に傾斜して測定するため、試料の傾斜方向、検出器との相対関係、SEMのスキャン方向などのパラメーターが最終的な方位決定のために重要な役割を果たしている。3次元の方位を示すEuler角の定義はBungeの表記法に則っていることが多くの場合測定の基準であるが<sup>[1][2][3]</sup>、その表記法も測定系の座標によって異なる場合がある。今回は測定系の座標とEuler角の関係をまとめて各々の測定系での解釈の仕方を整理した。特に六方晶や正方晶などの対称性の低い結晶での方位の解釈を中心にして、90度対称性と180度対称性および360度対称性での結果の違いを試みている。

#### 参考文献

1. Randle, V., and Engler, O., Texture Analysis, Macrotecture, Microtexture and Orientation Mapping, Taylor and Francis, 2000, ISBN 9056992244
2. Bunge, H.J. 1982. Texture Analysis in Materials Science -Mathematical Methods. Butterworths, London.
3. Bunge, 1993, Texture Analysis in Materials Science, ISBN 3-928815-18-4)

キーワード：オイラー角、EBSD

Keywords: Euler angle, EBSD

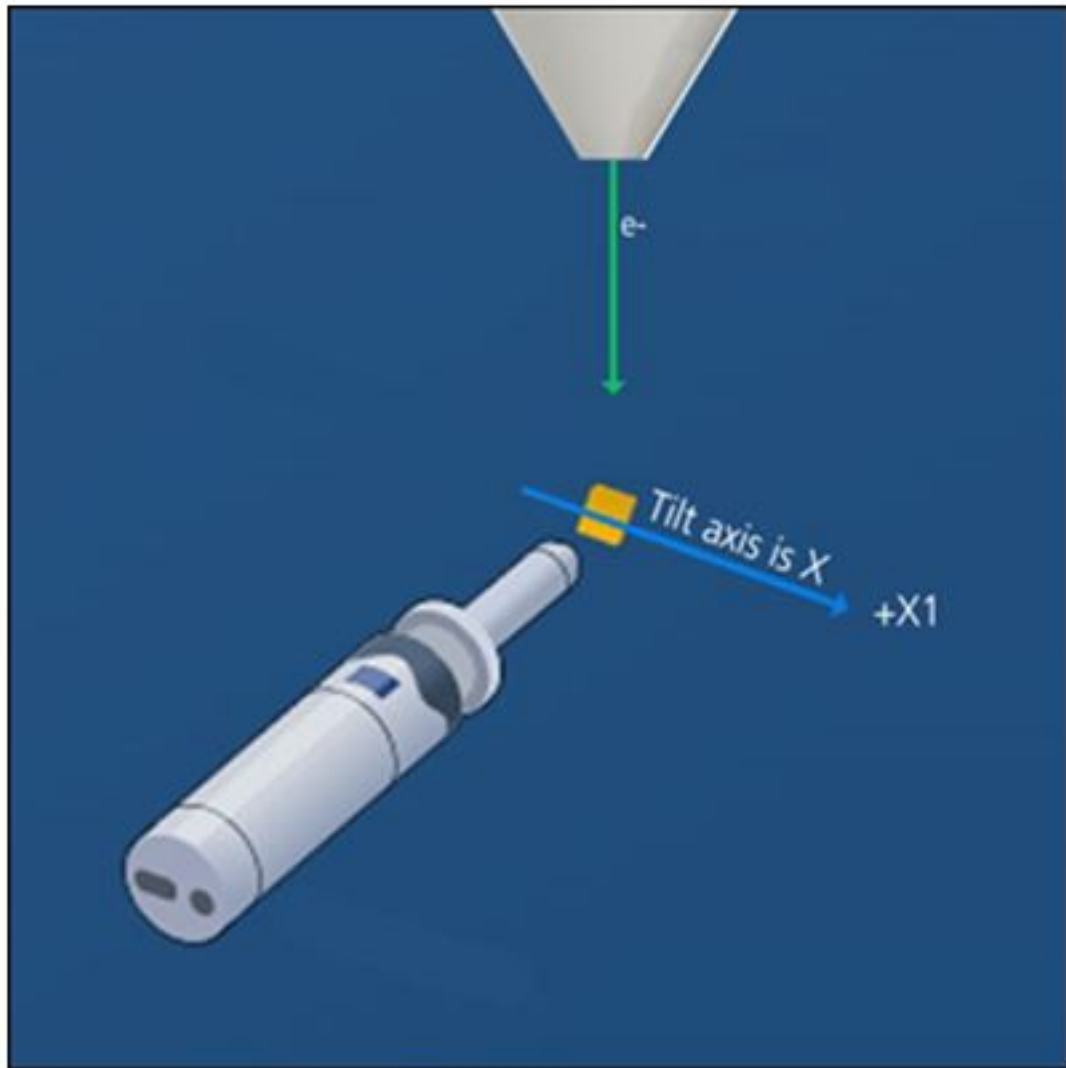


Fig.1 detector to sample direction

## 透過型電子顕微鏡を用いたタンパク質の結晶化における準安定相の直接観察

## Direct observation of metastable phase in protein crystallization using transmission electron microscopy

\*山崎 智也<sup>1</sup>、木村 勇気<sup>1</sup>\*Tomoya Yamazaki<sup>1</sup>, Yuki Kimura<sup>1</sup>

1.北海道大学低温科学研究所

1. Institute of Low Temperature Science Hokkaido University

A thermodynamically metastable phase, such as amorphous and dense liquid, has an important role in a crystallization process. In a nucleation process, amorphous particles appear before nucleation of a crystalline phase, and those serve as nucleation sites for more energetically favorable crystalline phases [1]. In crystal growth processes, a dense and liquid-like cluster most likely assists formation of a macro-step on a crystal surface [2]. To demonstrate these crystallization processes, *in situ* observation using a microscope is one of the powerful methods because it can directly visualize these processes in real time. However, it is difficult to visualize behavior of such metastable particles because those sizes are normally submicron, sometimes in nanoscale. Recently developed liquid cells adapting to high-vacuum environments of transmission electron microscopy (TEM) provide nanoscale views of nanoparticles and crystallization processes in aqueous solutions [3]. We developed the fluid-reaction transmission electron microscopy (FR-TEM) system for *in situ* observation of crystallization process in aqueous solutions. Using this system, we performed *in situ* observation of a protein crystallization, for investigating its nucleation and crystal growth processes.

Hen-egg white lysozyme was used as a protein sample without further purification and was crystallized using NaCl as a precipitant in a sodium acetate buffer solution at pH = 4.5. For observation of crystals in a solution under TEM, we used a "Poseidon" TEM holder (Protochip, Inc.) combined with a liquid cell. The liquid cell consists of a pair of semiconductor-based plates with an amorphous silicon nitride window and 150 or 500-nm-thick spacer to form a flow path of a crystallization solution.

We succeeded in observing two crystalline phases of orthorhombic and tetragonal in addition to an amorphous phase of the lysozyme [4]. Orthorhombic is the most stable of phases in our experimental solution. In this presentation, we present recent results of *in situ* TEM observation of its crystallization process including behaviors of metastable phases.

Acknowledgement

The authors acknowledge supports from a Grant-in-Aid for Research Activity Start-up from KAKENHI (26887001), for a grant for Young Scientists (A) from KAKENHI (24684033) and for a grant for Scientific Research (S) from KAKENHI (15H05731).

References

- [1] M. H. Nielsen *et al.*, *Science* 345 (2014), 1158.
- [2] M. Sleutel & A. E. S. Van Driessche, *Proc. Natl. Acad. Sci. U.S.A* 111 (2014), E546.
- [3] F. M. Ross, *Science* 350 (2015), 6267.
- [4] T. Yamazaki *et al.*, *Microsc. Microanal.* 21 (2015), 255.

キーワード："その場"観察、透過型電子顕微鏡、結晶化、溶液成長、リゾチーム

Keywords: In situ observation, Transmission electron microscopy, Crystallization, Solution growth, Lysozyme



塩素酸ナトリウム水溶液中の銀ナノ粒子円偏光光学捕捉により誘起されるキラル結晶化におけるキラリティの偏り

Chiral Bias in Chiral Crystallization Induced by Circularly Polarized Laser Trapping of Silver Nanoparticles in Sodium Chlorate Solution

\*新家 寛正<sup>1</sup>、杉山 輝樹<sup>2</sup>、田川 美穂<sup>3</sup>、村山 健太<sup>3</sup>、原田 俊太<sup>3</sup>、宇治原 徹<sup>3</sup>

\*Hiromasa Niinomi<sup>1</sup>, Teruki Sugiyama<sup>2</sup>, Miho Tagawa<sup>3</sup>, Kenta Murayama<sup>3</sup>, Shunta Harada<sup>3</sup>, Toru Ujihara<sup>3</sup>

1.国立大学法人千葉大学融合科学研究科附属分子キラリティ研究センター、2.台湾国立交通大学応用化学系および分子科学研究所、3.国立大学法人名古屋大学未来材料・システム研究所未来エレクトロニクス集積研究センター

1.Molecular Chirality Research Center, Graduate School of Advanced Integration Science, 2.Applied Chemistry and Institute of Molecular Science, Taiwan National Chiao Tung University, 3.Institute of Materials and Systems for Sustainability, Graduate School of Engineering, Nagoya University

Chiral crystallization, in which chirality emerges spontaneously in the course of crystallization, has been received attention from the viewpoint of emergence of chirality. Thus, the exploration of physical factors that induce a chiral bias in chiral crystallization provides implications for the origin of bihomochirality. Asymmetric interaction between circularly polarized light (CPL) and chiral compound, i.e. circular dichroism (CD), has been considered as a candidate for the origin of bihomochirality,[1]. Many previous studies on photosynthesis of chiral molecule have proven that asymmetric light-matter interaction induces slight chiral bias in enantiomeric ratio of reaction product, so far.[2] However, light-based chiral bias in chiral crystallization still remains unreported. Two conceivable reasons may exist: (1) CD is intrinsically small, (2) there is no investigation on chiral bias by CPL-induced chiral crystallization with a guarantee of optical field effect on nucleation. We overcome these difficulties by two strategies: (1) the plasmonic enhancement of CD [3] and (2) continuous-wave (CW) laser-induced nucleation [4]. In this presentation, we report the first demonstration of significant chiral bias in NaClO<sub>3</sub> chiral crystallization by irradiating a tightly-focused circularly polarized CW laser at the interface between air and a NaClO<sub>3</sub> solution containing plasmonic AgNPs.

A CW CPL green laser (532 nm, 940±5 mW, ellipticity >93%) was focused onto the air-liquid interface of the undersaturated NaClO<sub>3</sub> solution containing AgNPs by using a 60x objective lens (NA = 0.9) equipped on an inverted polarized light microscope. We repeated crystallization and chirality identification of the NaClO<sub>3</sub> crystal 100 times and 100 times by using *l*- and *r*-CPL, respectively. The number of the resulting enantiomorphs was counted.

As the result of the laser irradiation, crystallization occurred from the focal spot. The crystallization using *l*-CPL(*r*-CPL) yielded *l*-enantiomorph 42(65) times and *d*-enantiomorph 58(35) times, respectively, indicating that the *d*-(*l*-)enantiomorph was dominant over the *l*-(*d*-)enantiomorph. Namely, the "dominant" enantiomorph can be switchable by switching the handedness of incident CPL, i.e. the chiral bias is enantioselective. In total, the "dominant" enantiomorph crystallized 123 times out of 200 crystallization. This chiral bias is statistically significant because the number of the "dominant" enantiomorph deviates 99% interval of the binomial distribution  $B(n,p) = B(200,0.5)$ , where  $n$  is the number of trials and  $p$  is the probability that the "dominant" enantiomorph crystallizes out (Figure 1). This deviation demonstrates that the probability  $p$  is more than 0.5, i.e. the probability of the occurrence of each enantiomorph is no longer equal.

We found that the crystallization of NaClO<sub>3</sub> chiral crystal can be induced by the irradiation of tightly focused CPL laser (532 nm) at the interface between air and NaClO<sub>3</sub> solution containing

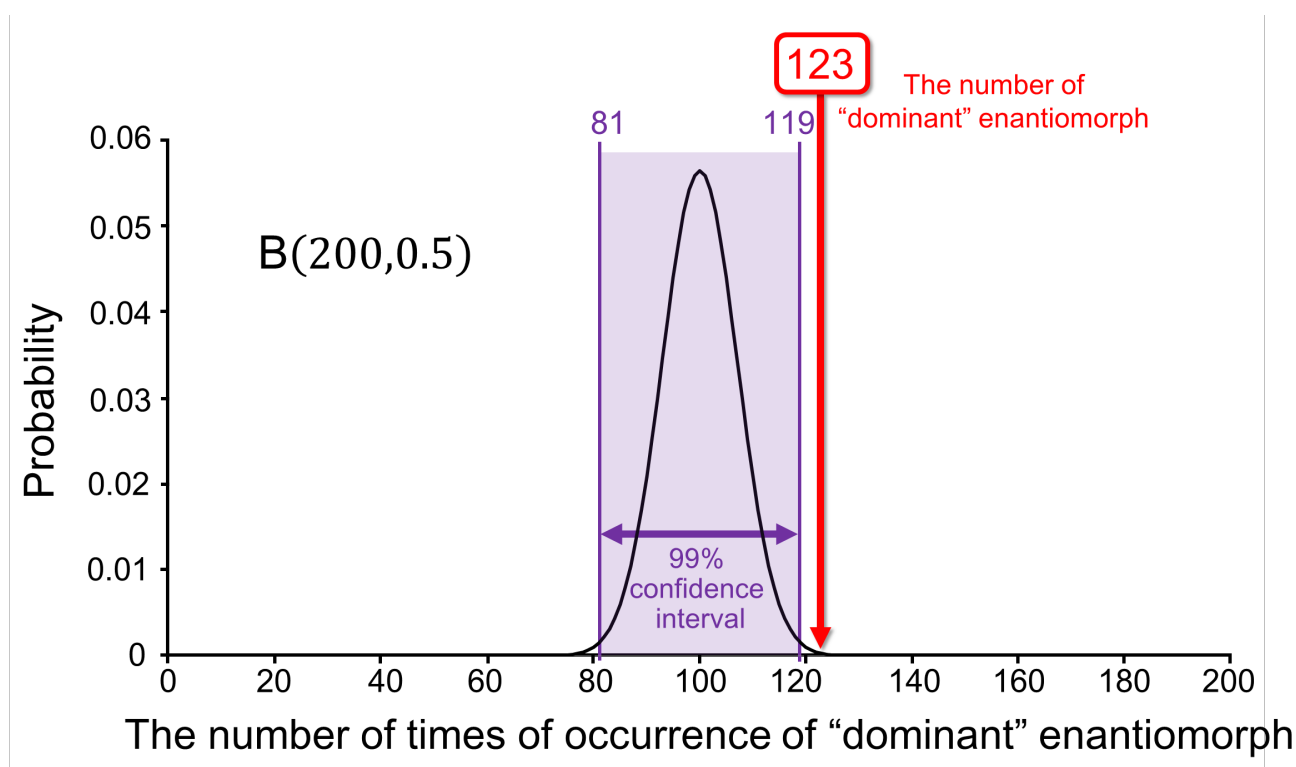


AgNPs. We also found that this crystallization method can cause a statistically-significant chiral bias in the probability of crystallization of both of the enantiomorphs. Moreover, the “dominant” enantiomorph is found to be switchable by changing the handedness of CPL. Our results may provide implications for the origin of bihomochirality.

- [1] W. A. Bonner, *Orig. Life Evol. Biosph.* 21(2), (1991), 59.  
 [2] B. L. Feringa, R. A. v. Delden, *Angew. Chem. Int. Ed.* 38, (1999), 3418.  
 [3] Y. Zhang, C. Gu, A. M. Schwartzberg, S. Chen and J. Z. Zhang, *Phys. Rev. B* 73, (2006), 165405.  
 [4] T. Sugiyama, T. Adachi, H. Masuhara, *Chem. Lett.* 36(12), (2007), 1480.

キーワード：キラル結晶化、レーザー誘起結晶化、円偏光、金属ナノ粒子、局在型表面プラズモン

Keywords: chiral crystallization, laser-induced crystallization, circularly polarized light, metal nanoparticle, localized surface plasmon



## 結晶の成長と溶解およびその形態

## Formation of patterns in growth and dissolution of crystals

\*横山 悦郎<sup>1</sup>\*Etsuro Yokoyama<sup>1</sup>

1. 学習院大学計算機センター

1. Computer Centre Gakushuin University

This talk is concerned with fundamental aspects of formation of pattern of crystals in undersaturation. The formation of patterns in crystal growth is a free-boundary problem in which the interface that separates the crystal from an associated solution or vapor phase moves under the influence of non-equilibrium conditions. The formation of patterns in crystal dissolution/evaporation is also a free-boundary problem. The topics of dissolution/evaporation pattern of crystals, however, have been neglected in comparison with the study of growth morphology of crystals except a few studies [1].

The growth patterns depend markedly on conditions in the solution/vapor phase, such as temperature and concentration, which influence the growth speed of each element of the interface. The growth speed of the interface also depends on the local geometry of the interface, specifically on the interface curvature and the orientation of the interface relative to the crystal axes. Although the dissolution/evaporation forms diminish with time, the patterns could also depend on conditions in the solution/vapor phase under the small deviation from equilibrium conditions.

The local motions of interface can, in principle, be determined by solving the transport equations that take into account the following elementary processes:

- 1) a diffusion process for the transport of latent heat liberated or absorbed at the interface,
- 2) a process for diffusing molecules through the solution/vapor phase toward or from the interface, and
- 3) an interface kinetic process for incorporating/decorporation molecules into/from a crystalline phase at the interface[2].

We consider the asymmetry of normal speed at interface relative to the equilibrium point from supersaturation to undersaturation. We shall term the positive normal speed the growth rate of crystallization and the negative normal speed the dissolution/evaporation rate. Both local normal speed  $V$  of the interface can be proportional to the deviation from local equilibrium conditions  $\Delta$ , which depend on interface curvature:

$$V = \beta \Delta,$$

where  $\beta$  is a kinetic coefficient that can depend on interface orientation and the degree of supersaturation or undersaturation at the interface. In general,  $V$  includes the Boltzmann factor  $\exp(-E/kT)$ , where  $E$  is an activation energy,  $k$  is the Boltzmann constant and  $T$  is temperature. Since the factor  $\exp(-E/kT)$  causes enhancement of the dissolution/evaporation rate for  $T > T_e$  but reduction of the growth rate for  $T < T_e$ , the behavior of  $V$  relative to  $T_e$  is asymmetric. On the other hand if  $V$  is controlled by the undersaturation and the factor  $\exp(-E/kT)$  does not work, the dissolution rate can approach a limiting value. This is because the degree of undersaturation has a minimum limit, e.g., pure solvent without solute.

In this talk, we show the patterns during growth or dissolution/evaporation of a two-dimensional crystal under conditions such that the transport of heat and/or solute is so rapid that growth is controlled by interfacial processes. Furthermore, we discuss the formation of both patterns in the point of view of the asymmetry of normal speed at interface relative to the equilibrium point.

## references

- [1] R. Lacmann, W. Franke and R. Heimann, *J. Crystal Growth*, 26(1974)107–116; R. Lacmann, R. Heimann and W. Franke, *J. Crystal Growth*, 26(1974)117–121; W. Franke, R. Heimann and R. Lacmann, *J. Crystal Growth*, 26(1974)145–150.
- [2] J. P. Hirth and G. M. Pound, *J. Chem. Phys.*, 26(1957)1216–1224; J. P. Hirth and G. M. Pound, *Acta Metallurgica*, 5(1957)649–653; J. P. Hirth and G. M. Pound, *J. Phys. Chem.*, 64(1960)619–626; J. P. Hirth and G. M. Pound, *Condensation and evaporation, Nucleation and Growth kinetics*, *Progress in Material Science* 11, Editor B. Chalmers, Pergamon Press 1963.

## 結晶の成長と溶解の複合

## The Coupled Dissolution and Growth

\*塚本 勝男<sup>1</sup>\*Katsuo Tsukamoto<sup>1</sup>

1.大阪大学大学院工学研究科

1.Graduate School of Engineering, Osaka University

Lots of discussions on whether growth is an opposite phenomena of dissolution or not. Here after presenting the real rates observed in-situ in both cases at the same absolute value of chemical potential, we show the difference. This may lead to a deeper understanding of coupled dissolution and growth of crystals in solution. We will show even in dissolution process of a crystal crystallization barrier plays an important role.

キーワード：溶解、結晶成長、メカニズム

Keywords: dissolution, growth, mechansim

## NaCl単結晶の表面自由エネルギー密度とラフニング転移

## Specific Surface Free Energy and Roughening Transition of Sodium Chloride Single Crystal

\*丸山 諒也<sup>1</sup>、鈴木 孝臣<sup>1</sup>\*Ryoya Maruyama<sup>1</sup>, Takaomi Suzuki<sup>1</sup>

1.信州大学大学院総合理工学研究科

1.Graduate School of Science and Engineering, Shinshu University

Specific surface free energy (SSFE) is one of important values to discuss the morphology and growth of crystal, and theoretically well discussed. However, experimental trial to determine the SSFE of crystal is very few. We have already measured contact angle of liquids on crystals, for example, apatite, ruby, and quartz in order to determine the SSFE. The SSFE of crystals were proportional to growth rate of crystals, which qualitatively satisfy Wulff's relationship. Experimentally determined SSFE is not that of ideal flat face, but it includes step free energy. This time we tried to measure the step free energy of sodium chloride and discussed the roughness of crystal face.

Sodium chloride single crystal was synthesized by evaporation of saturated water solvent keeping at 40°C. Cubic crystal with (100) face was obtained. Octahedral sodium chloride single crystal with (111) face was also synthesized from water solvent with 15% of formamide keeping also at 40 °C. Crystals was heated by electric furnace at 600°C and kept for 1 hour.

Droplets of ethylene glycol or diethylene glycol with volume of 0.1μL were dropped on the crystal surface using a micropipette. The contact angle were observed using digital camera.

SSFE were calculated by Wu's harmonic mean equation and Fowkes approximation. The calculated value of SSFE of (100) surface before and after heat treatment were 45.9, 48.8mN/m, and SSFE of (111) face before and after heat treatment were 37.9 and 38.9mN/m. The SSFE was increased by heat treatment for (100) and (111) face. Because the observed SSFE contains step free energy, the increase of SSFE is caused by increase of steps on the crystal face. The increase of SSFE was observed after the heat treatment at 600°C. Therefore, the roughening temperature is considered to exist at the temperature under 600°C.

キーワード：表面自由エネルギー密度、NaCl単結晶、ラフニング転移

Keywords: specific surface free energy, sodium chloride single crystal, roughening transition

## 液相からの気泡核生成の大規模分子動力学計算による気泡表面張力の算出

## Surface energy of bubbles evaluated by large-scale molecular dynamics simulations of homogeneous bubble nucleation

\*田中 今日子<sup>1</sup>、田中 秀和<sup>2</sup>、アンジェリル レイモンド<sup>3</sup>、ユルグ ディアモンド<sup>3</sup>\*Kyoko Tanaka<sup>1</sup>, Hidekazu Tanaka<sup>2</sup>, Angelil Raymond<sup>3</sup>, Juerg Diemand<sup>3</sup>

1.北海道大学低温科学研究所、2.東北大学、3.チューリッヒ大学

1.Institute of Low Temperature Science, Hokkaido University, 2.Tohoku University, 3.Univ. of Zurich

液体からの気泡生成は様々な分野に関わる重要な現象のひとつであるが、その気泡の核生成過程についての理解は未だ限られている。古典的核形成理論は、核形成過程の巨視的記述を与え広く用いられているが、理論から得られる核生成率は実験や分子動力学(MD)シミュレーションからの得られる核生成率と大きくずれることが指摘されている。例えば、従来のMD計算から得られた気泡の生成率は古典的理論と比較すると、ほとんどの場合において古典的理論の核生成率よりも3桁から20桁程度も高くなる結果が得られているが、その原因は未だ明らかではない [1]。我々は LAMMPS を用いて 5 億体のレナードジョーンズ(LJ)分子から成る液相からの気泡核生成の分子動力学(MD)計算を行った。温度は $T/(\epsilon/k) = T^* = 0.6 - 0.86$  ( $\epsilon$ はLJ系のエネルギー単位, $k$ はボルツマン係数)、圧力  $P$  は  $-300 < P/P_{eq} < 0.5$  ( $P_{eq}$ は平衡蒸気圧)のさまざまな範囲において、NVE系のもとで気泡が生成し成長する様子を観察した。従来のMD計算の多くは初めの気泡が形成される時間から核生成率を見積もる MFPT 法(the mean first passagetimes)が用いられてきたが、本研究では複数の気泡の発生から核生成率を求める方法(Yasuoka-Matsumoto method)を用いて正確に核生成率を求めることに成功した。また気泡のサイズ分布から気泡生成のための自由エネルギーの算出や気泡の物理的性質など詳細な解析を行った

[1,2]。我々が得た核生成率は、古典的理論から得た値と高温で一致する一方、低温では大きくずれ、理論値より大きくなる。この古典的理論とのずれは以下のように説明される。従来の理論では核生成率 $J$ の表式は $J = J_0 \exp(-G/kT)$ であり、プレファクター $J_0$ は液体圧力に依らない一定の値とされてきた(但し、 $G$ は核生成の自由エネルギー)。しかし一方で、 $J_0$ は臨界核付近での気泡の成長率により決定し、液体圧力に大きく依存することが指摘されている[3]。とくに液体圧力と平衡圧力の差が十分大きい場合には、気泡の周りの流体の慣性や粘性が効き、上記のプレファクターと数桁異なる[4]。正確なプレファクターを用いて得られた核生成理論とMD計算を比較することによりナノサイズの気泡の表面張力を算出できる。これら2つの古典的理論の改良により多くのMD計算や実験が説明可能である。

[1] J. Diemand et al., Phys. Rev. E, 90, 052407 (2014).

[2] R. Angelil et al., Phys. Rev. E, 90, 063301 (2014).

[3] Y. Kagan, Russ. J. Phys. Chem. 34, 42 (1960).

[4] K. K. Tanaka et al., Phys. Rev. E, 92, 022401 (2015).

キーワード：気泡核生成、表面エネルギー、ナノ粒子、分子動力学計算

Keywords: bubble nucleation, surface energy, nano particle, molecular dynamics simulation

## 微小重力下におけるアルミナの均一核生成過程の赤外スペクトルその場測定

In-situ IR measurement in homogeneous nucleation process of alumina under  $\mu\text{G}$  environment\*石塚 紳之介<sup>1</sup>、木村 勇気<sup>1</sup>、山崎 智也<sup>1</sup>、左近 樹<sup>2</sup>、稲富 裕光<sup>3</sup>\*Shinnosuke Ishizuka<sup>1</sup>, Yuki Kimura<sup>1</sup>, Tomoya Yamazaki<sup>1</sup>, Itsuki Sakon<sup>2</sup>, Yuko Inatomi<sup>3</sup>

1.北海道大学低温科学研究所、2.東京大学大学院理学研究科、3.宇宙航空研究開発機構

1.Institute of Low Temperature Science, Hokkaido University, 2.Graduate School of Science, University of Tokyo, 3.Japan Aerospace Exploration Agency

Homogeneous nucleation process from vapor is characterized by the ratio between time scales for supersaturation increase and for source collision expressed as  $\Lambda$ [1]. Under the physical condition with the same  $\Lambda$  value, homogeneous nucleation process has been regarded to follow the same process. At the dust forming front around evolved stars,  $\Lambda$  value has been calculated to be  $\sim 10^{3-5}$  from total pressure and velocity of stellar wind. In contrast,  $\Lambda$  value of  $\sim 10^{0-2}$  is known for the gas evaporation method which is one of the simplest experimental methods to produce dust analogues via homogeneous nucleation [2, 3].

In-situ IR measurement during nucleation of nanoparticles in the gas evaporation method proved multi-step formation of metal oxide from vapor to crystalline via liquid droplet in our ground based experiment [4]. Using our advanced technique, we measured IR spectra of nucleating alumina and its evolution while nanoparticles are free-flying under  $\mu\text{G}$  environment in which  $\Lambda$  approximates to the value at dust formation region. Specially designed experimental apparatus equipped with dispersive IR spectrometer was loaded to S-520-30 sounding rocket by which the apparatus carried to altitude of 312 km. We also performed ground based experiment combined with FT-IR.

IR spectra of nucleating alumina measured in ground based experiment showed broad absorption extending  $>11 \mu\text{m}$ . Formed nanoparticles were observed by TEM and identified to  $\delta$ -alumina. In contrast, sharp absorption centered at  $13 \mu\text{m}$  was appeared in  $\mu\text{G}$  experiment. This  $13 \mu\text{m}$  band is one of the most indicative features of corundum ( $\alpha$ -alumina) sphere. Corundum is the most plausible candidate for the origin of unidentified  $13 \mu\text{m}$  feature which is often observed for oxygen rich AGB stars with low-mass loss rate [5, 6]. Polymorphic behavior of alumina in homogeneous nucleation process at different  $\Lambda$  will be the key to understand astronomical dust formation.

## Reference

- [1] Yamamoto, T. & Hasegawa, H., 1977 Progress of Theoretical Physics, Vol. 58, No. 3, 816
- [2] Kimura, Y., Miura, H., Tsukamoto, K., Li, C. et al., 2011, J. Cryst. Growth, 316, 196
- [3] Kimura, Y., Tanaka, K. K., Miura, H. & Tsukamoto, K., 2012, Crystal Growth & Design, 12(6), 3278-3284.
- [4] Ishizuka, S., Kimura, Y. & Sakon, I., 2015, The Astrophysical Journal, 803 (2), 88.
- [5] Speck, A. K., Barlow, M. J., Sylvester, R. J. & Hofmeister, A. M., 2000, Astronomy and Astrophysics Supplement Series, 146(3), 437-464.
- [6] Sloan, G. C., Kraemer, K. E., Goebel, J. H. & Price, S. D., 2003, The Astrophysical Journal, 594(1), 483.

## 糖、塩、アミノ酸を添加した系における氷の粒成長

Grain growth of ice from aqueous solutions of sugars, salts and amino acids

\*嶋田 達郎<sup>1</sup>、鍵 裕之<sup>1</sup>、小松 一生<sup>1</sup>、石橋 秀巳<sup>2</sup>、前田 竜郎<sup>3</sup>\*Tatsuro Shimada<sup>1</sup>, Hiroyuki Kagi<sup>1</sup>, Kazuki Komatsu<sup>1</sup>, Hidemi Ishibashi<sup>2</sup>, Tatsuro Maeda<sup>3</sup>

1. 東京大学大学院理学系研究科附属地殻化学実験施設、2. 静岡大学理学部地球科学科、3. 日清フーズ

1. Geochemical Research Center, Graduate School of Science, University of Tokyo, 2. Department of Geoscience, Shizuoka University, 3. Nisshin Foods

## Introduction

Salts and organic matters exist in icy bodies and comets. Chemical evolution from simple molecules to more complex organic compounds is a hot issue concerning the origin of life. Mixtures of ice and organic matters can play an important role for chemical evolution. Sugahara and Mimura (2015) conducted shock experiments on a mixture of alanine, ice, and silicate under cryogenic conditions simulating comet impacts and reported the oligomerization of alanine. For precise understanding of the reaction, it is necessary to observe morphology of ice including organic matters at low temperature. Effects of salts, amino acid and sugar to morphology and grain growth of ice are important research targets for food science as well as planetary science. In this study, we investigate grain-growth kinetics of ice crystallized from salt, sugar or amino-acid solutions from in-situ optical observations at low temperature.

## Experimental procedure

Pure water, NaCl solutions, amino-acid (aspartic acid and glutamic acid) solutions and sugar (glucose, sucrose, maltose, maltotriose and maltotetraose) solutions were prepared as samples. These sample solutions were set between two cover glasses with a gap of ~40  $\mu\text{m}$  on a heating-cooling stage and sample chamber was filled with dry nitrogen gas. These sample solutions were rapidly cooled to  $-30\text{ }^\circ\text{C}$  at a rate of  $10\text{ }^\circ\text{C}/\text{min}$ . After the samples were frozen, the sample temperature was increased at a rate of  $10\text{ }^\circ\text{C}/\text{min}$  and was kept for 300 min at  $-5\text{ }^\circ\text{C}$ . Optical images and movies were collected in situ under a polarizing microscope with crossed nicols. Phase identifications were conducted by Raman spectroscopy.

## Results and Discussion

Figure 1 shows representative optical photographs of ices after 300 minutes reaching at  $-5\text{ }^\circ\text{C}$ . All solutions froze into aggregates of fine ice crystals in a moment before reaching at  $-30\text{ }^\circ\text{C}$ . In pure water, no homogenous grain growth was observed after 300 min at  $-5\text{ }^\circ\text{C}$ , but abnormal grain growth up to approximately 50  $\mu\text{m}$  was observed. In the case of a salt solution, after reaching at  $-5\text{ }^\circ\text{C}$ , ice grains grew to a homogeneous size of 35  $\mu\text{m}$  in average and the solution existed in triple junctions between ice crystals. In amino acid solutions, notable grain growth was not observed and fine grains remained. The abnormal grain growth similar to the case of pure water was observed in some cases of amino acids. Moreover, grain-growth rate in amino acid system was much lower than the case of pure water. This result suggests that amino acid inhibits grain growth of ice. In sugar solutions, when number of carbon ring changed from 2 to 4, appearances of samples changed drastically.

This study confirmed that morphology and grain-growth kinetics of ice are strongly affected by chemical composition of starting solutions. These results are useful to understand chemical reactions occurring in ice and will contribute to improve frozen preservation of foods.

キーワード：糖、塩、アミノ酸、粒成長、その場観察



Keywords: sugars, salts, amino-acids, grain growth, observation in situ

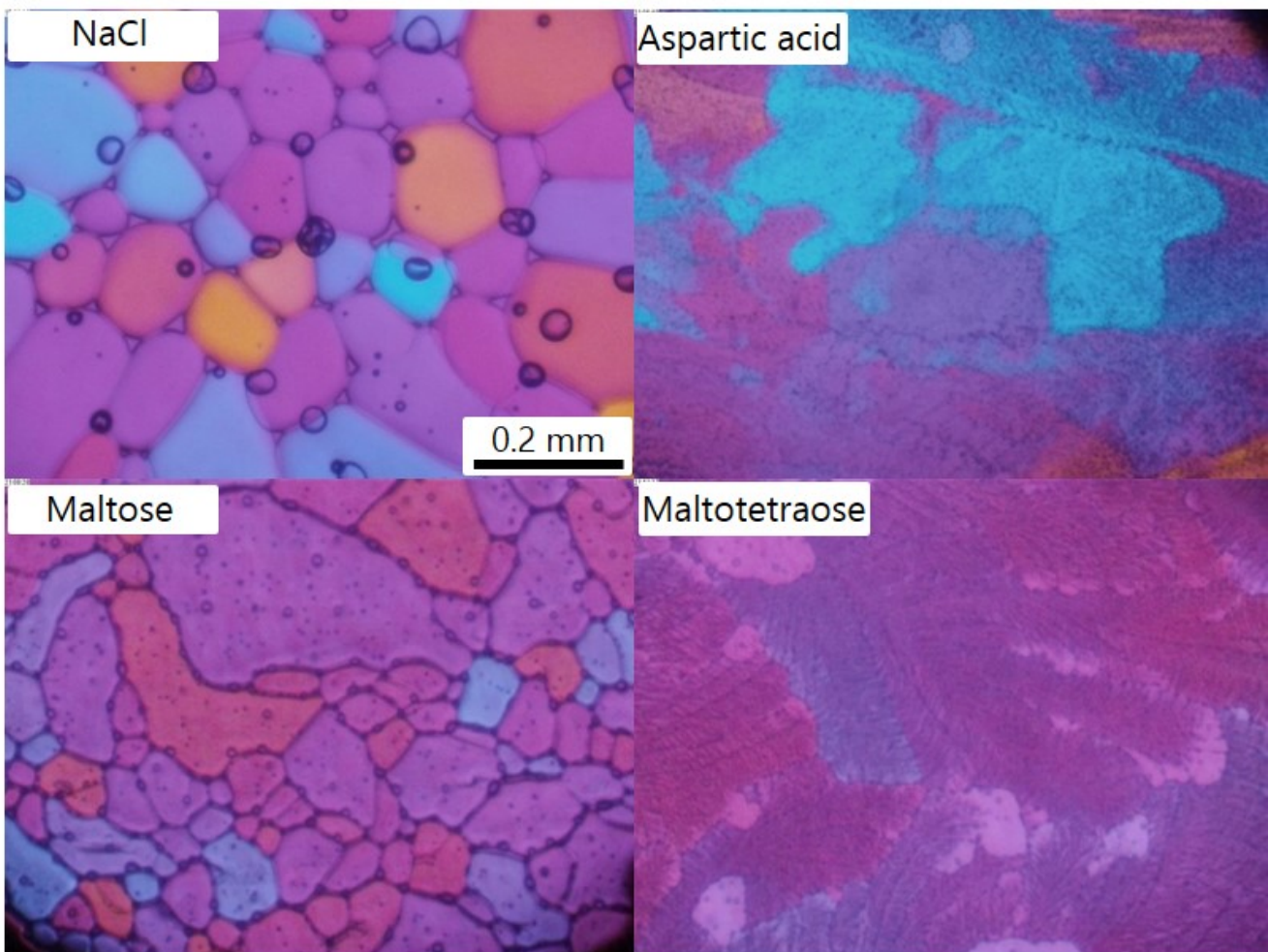


Figure 1. Representative optical images (crossed nicols) of ice crystals obtained 300 min after reaching at  $-5\text{ }^{\circ}\text{C}$ . The contrasts of these images depend on crystal orientations.

## 結晶成長におけるヒステリシスの再現

## Reproduction of hysteresis in crystal growth

\*三浦 均<sup>1</sup>\*Hitoshi Miura<sup>1</sup>

1.名古屋市立大学大学院システム自然科学研究科

1. Graduate School of Natural Sciences, Department of Information and Biological Sciences, Nagoya City University

ステップ・ダイナミクスは、結晶成長における本質的な物理過程のひとつである。結晶表面には原子スケールの高さを持つ段差（ステップ）が存在し、そこに原子や分子が取り込まれることによってステップが前進し、結晶が一層ずつ積み上げられていく（層成長モデル）。従って、結晶成長メカニズムを解明するには、ステップの供給メカニズムやステップ前進速度を決める物理を理解する必要がある。

ステップ・ダイナミクスは、不純物の存在によって大きく影響を受ける。成長ヒステリシスは、不純物の存在によって引き起こされる良く知られた現象のひとつである[e.g., 1]。例えば、溶液からの結晶成長の場合、一般的に結晶成長速度は溶液の過飽和度と正の相関がある。しかし、溶液に不純物が含まれている場合、過飽和度を徐々に減少させながら成長速度を測定した場合と、逆に増加させながら測定した場合とでは、ある過飽和度における成長速度の値が異なる場合がある。この履歴現象は、結晶表面に吸着した不純物によってステップ前進が阻害される効果と、ステップが頻繁に結晶表面を掃くことで不純物の吸着が抑制される効果の相互作用によって引き起こされると考えられてきた。成長ヒステリシスに関する従来の理論では、吸着不純物密度やステップ前進速度などの物理量を時間・空間的に平均化して扱っていた（平均場理論, [e.g., 2-4]）。しかし、実際にはこれらの量は結晶面上の場所によって異なり、かつ時間とともに変化するため、平均場理論が実際の系にそのまま適用できるかどうかは自明ではなかった。

本講演では、不純物脱離・吸着過程を考慮したステップ・ダイナミクスの数値計算によって、成長ヒステリシスを再現した成果[5]について報告する。我々は近年、ステップ・ダイナミクスをフェーズ・フィールド（PF）法に基づいて定量的に扱う手法を開発した [6,7]。これに加えて、不純物脱離・吸着過程をモンテカルロ法（MC）法で計算することにより、吸着不純物密度やステップ前進速度などの物理量の時間・空間的变化を模擬した。高過飽和度・吸着不純物なしの状態から計算を開始し、一定の率で過飽和度を低下させ、その後増加させるというサイクルを10回繰り返してステップ前進速度の変化を調べたところ、いずれのサイクルにおいても成長ヒステリシスが現れることを確認した。過飽和度減少時と増加時のステップ前進速度履歴をそれぞれ10サイクル分平均したところ、平均場理論の結果[3]とよく一致することが分かった。以上の結果は、数値計算によって成長ヒステリシスを再現した初めての成果である。本提案手法を応用することで、結晶成長における不純物効果の理解が飛躍的に発展することが期待できる。

参考文献：[1] R. W. Friddle et al. (2010), PNAS 107, 11. [2] Y. O. Punin and O. I. Artamonova (1989), Kristallografiya 34, 1262. [3] H. Miura and K. Tsukamoto (2013), Cryst. Growth Des. 13, 3588. [4] H. Miura and K. Tsukamoto (2013), Japan Geoscience Union Meeting 2013, abstract MIS31-P05. [5] H. Miura (2016), accepted for publication in Cryst. Growth Des. [6] H. Miura and R. Kobayashi (2015), Cryst. Growth Des. 15, 2165. [7] H. Miura (2015), Cryst. Growth Des. 15, 4142.

キーワード：結晶成長、ステップ・ダイナミクス、不純物、ヒステリシス

Keywords: Crystal growth, Step dynamics, Impurity, Hysteresis

## サイズ分布を考慮したモンモリロナイト溶解の数値計算

## Numerical calculation of montmorillonite dissolution in consideration of the size distribution

\*窪川 浩太<sup>1</sup>、三浦 均<sup>1</sup>、佐藤 久夫<sup>2</sup>、山口 耕平<sup>3</sup>\*Kota Kubokawa<sup>1</sup>, Hitoshi Miura<sup>1</sup>, Hisao Satoh<sup>2</sup>, Kohei Yamaguchi<sup>3</sup>

1.名古屋市立大学大学院システム自然科学科、2.三菱マテリアル株式会社エネルギー事業センター那珂エネルギー開発研究所、3.三菱マテリアル株式会社

1. Graduate School of Natural Sciences, Department of Information and Biological Sciences, Nagoya City University, 2. Naka Energy Research Laboratory, Mitsubishi Materials Corporation, 3. Mitsubishi Materials Corporation

近年、原子力発電所の利用に伴って生じた多量の放射性廃棄物の処分方法が課題となっている。我が国では、実現可能な処分手法として、「地層処分」が検討されている。地層処分とは、高レベル放射性廃棄物をガラス固化体にし、鉄製の容器に入れ、これをベントナイトという粘土鉱物(モンモリロナイト)を主成分とする緩衝材で覆い、地下数百メートルよりも深い場所に処分することである。モンモリロナイトは、水に接すると膨張し、止水する機能を持つ。しかし、数万年に及ぶ長期間における保存においては、モンモリロナイトが地下水と反応して溶解し、止水性としての機能が損なわれた結果、内部の放射性物質が地下水によって流出する危険性がある。したがって、長期の安定保存の為に、モンモリロナイトの溶解挙動を予想することは極めて重要である。

本研究では、モンモリロナイトの溶解挙動を調べるため、数値計算手法を用いたシミュレーションを行った。閉鎖的環境下でアルカリ性溶液にさらされた様々なサイズのモンモリロナイト粒子を想定し、溶解に伴う各粒子のサイズ変化と溶液の濃度変化を同時に計算した。粒子の溶解速度式には、過飽和度依存性とギブス・トムソン効果による粒子サイズ依存性を考慮した。溶液が未飽和な場合の溶解速度式には溶解実験で得られた経験式を用い、溶液が過飽和になった場合の成長速度式には溶解速度式の符号を逆にした式を仮定した[1]。溶液の過飽和度はPHREEQC[2]を用いて計算した。また、従来の研究ではほとんど考慮されていなかったサイズ分布の違いによる差にも着目した。初期の粒子サイズ分布として、一様分布、対数一様分布、正規分布、対数正規分布の4種類を想定した。

対数正規分布を持つ粒子を未飽和溶液と反応させた場合、計算初期は全サイズの粒子が溶解し、溶液の未飽和度が小さくなっていき、やがてほぼ飽和状態となった。ほぼ飽和になった状態では、ギブス・トムソン効果により、小さい粒子は溶解し、大きい粒子が成長に転じる様子が確認された。大きな粒子が成長に転じるまでに要する期間は、計算初期における溶液体積に対する全粒子体積の比(固液体積比)に依存した。固液体積比が $10^{-5}$ の場合は、計算開始から約7000年後に成長に転じた。固液体積比を大きくすると、成長に転じるまでに要する期間が約10~100年まで短縮されることが分かった。また、成長に転じるサイズの下限值も、固液体積比の増加と共に大きくなることが分かった。以上、サイズ分布を考慮したモンモリロナイト粒子溶解過程の数値計算により、長期の安定保存にはギブス・トムソン効果を考慮することが重要であることが示唆された。

参考文献: [1] Cama et al. (2000), *Geochem. Cosmochim. Acta* 64, 2701. [2] PHREEQC -A Computer Program for Speciation, Batch-Reaction, One-Dimensional Transport, and Inverse Geochemical Calculations. [http://wwwbrr.cr.usgs.gov/projects/GWC\\_coupled/phreeqc/](http://wwwbrr.cr.usgs.gov/projects/GWC_coupled/phreeqc/).

## 観測ロケットS-520-30号機を用いたアルミナとシリカの気相からの核生成実験

## Nucleation experiment of alumina and silica from vapor phase using the sounding rocket S-520-30

\*木村 勇気<sup>1</sup>、石塚 紳之介<sup>1</sup>、山崎 智也<sup>1</sup>、田中 今日子<sup>1</sup>、竹内 伸介<sup>2</sup>、稲富 裕光<sup>2</sup>

\*Yuki Kimura<sup>1</sup>, Shinnosuke Ishizuka<sup>1</sup>, Tomoya Yamazaki<sup>1</sup>, Kyoko Tanaka<sup>1</sup>, Shinsuke Takeuchi<sup>2</sup>, Yuko Inatomi<sup>2</sup>

1.北海道大学低温科学研究所、2.宇宙航空研究開発機構宇宙科学研究所

1.Institute of Low Temperature Science, Hokkaido University, 2.JAXA/ISAS

Nucleation event determines the condensation sequence, number density, size, morphology and crystalline structure of cosmic dust particle, called dust, in a gas outflow of dying stars or a gas plume after shock wave heating in the primitive solar nebula. Using nucleation theories, such characters of dust have been expected. However, it has been well known that results obtained by classical nucleation theory and by experiments have a large difference each other. We believe that one of the reasons is the difference of physical parameters of nanometer sized particles from its bulk. Although nucleation is a process progressed in nanometer scale, physical parameters of bulk materials have been used. To determine the physical parameters of nanoparticles, we constructed an in-situ observation system of temperature and concentration during homogeneous nucleation in vapor phase using interferometry in the laboratory.

Nanoparticles are formed as dust analogues from a supersaturated vapor after evaporation of the starting material by electrical heating in a gas atmosphere. Using the specially designed double-wavelength Mach-Zehnder-type laser interferometer, nucleation temperature and partial pressure can be obtained simultaneously. Then, surface free energy and sticking probability can be determined using timescale for cooling based on nucleation theories (Kimura et al. 2012). In case of laboratory experiment, convection of gas atmosphere caused by thermal heating generates heterogeneity of nucleation environment, such as temperature and concentration profiles around evaporation source. In microgravity, evaporated vapor diffuses uniformly and the temperature profile becomes concentric around the evaporation source. As the result, nucleation will occur at the same condition. In addition, microgravity condition allow us to duplicate the ratio of timescale for cooling and collision frequency of vapor around supernovae and asymptotic giant branch stars. Therefore, we performed microgravity experiments using the sounding rocket S-520-30 launched on September 11<sup>th</sup>, 2015.

Two same experimental systems, which construct with the interferometer, nucleation chamber and camera recording modules were designed to fit the size and weight limitation and installed into the nosecone of the rocket. The evaporation source and gas atmosphere are silica and argon ( $4 \times 10^4$  Pa) for silica dust, and alumina and a gas mixture of oxygen ( $2 \times 10^3$  Pa) and argon ( $3.8 \times 10^4$  Pa) for alumina dust. The experiments were run sequentially and automatically started after launch of the rocket. The evaporation sources of silica and aluminum were electrically heated in the gas atmosphere under microgravity. Evaporated vapor was diffused, cooled and nucleated in the gas atmosphere. The temperature and concentration at the nucleation site can be determined from the movement of the interference fringes. Here, we will show the results of the experiments including supersaturation ratio, and the physical properties of those nanoparticles.

キーワード：微小重力、ダスト、核生成

Keywords: Microgravity, Dust, Nucleation



## 溶解/成長する炭酸カルシウム近傍におけるpH変化の可視化の試み

Visualization of pH change around calcium carbonate crystals during dissolution and growth

\*川野 潤<sup>1</sup>、豊福 高志<sup>2</sup>、長井 裕季子<sup>2</sup>、河田 佐知子<sup>2</sup>、板垣 璃沙<sup>1</sup>、永井 隆哉<sup>1</sup>\*Jun Kawano<sup>1</sup>, Takashi Toyofuku<sup>2</sup>, Yukiko Nagai<sup>2</sup>, Sachiko Kawada<sup>2</sup>, Risa Itagaki<sup>1</sup>, Takaya Nagai<sup>1</sup>

1.北海道大学大学院 理学研究院、2.海洋研究開発機構

1.Faculty of Science, Hokkaido University, 2.JAMSTEC

For the investigation of the growth and dissolution of calcium carbonate,  $\text{CaCO}_3$ , it is important to understand how carbonate and bicarbonate ions behave in these processes. The pH monitoring of a solution during  $\text{CaCO}_3$  growth or dissolution is a useful technique for this purpose, and actually in a number of the previous studies, the pH measurements of bulk solution during the growth have been performed. However, to clarify the detail process on the surface, especially the behavior of bicarbonate ions, regional change of pH just above the crystal surface should be monitored. Recently, we have started an attempt to visualize the distribution of pH around  $\text{CaCO}_3$  crystals which inorganically grows or dissolves, by applying the method used for the research on the biogenic calcification of foraminifers. We have succeeded to detect the pH change near a dissolved calcite surface, which may provide new insights into both inorganic and biogenic formation mechanism of  $\text{CaCO}_3$ .

キーワード：炭酸カルシウム、溶解、pH

Keywords: calcium carbonate, dissolution, pH

## 粘土の固化過程の結晶成長：スメクタイトのゼオライト化反応

Crystal growth in clay solidification: zeolitization of smectite

\*佐藤 久夫<sup>1</sup>\*Hisao Satoh<sup>1</sup>

1.三菱マテリアル株式会社エネルギー事業センター那珂エネルギー開発研究所

1.Naka Energy Research Laboratory, Mitsubishi Materials Corporation

地球表層では、造岩鉱物は水との反応により、微細な粘土鉱物へと風化する。微細な粘土鉱物は表層環境では土壌として安定に存在し続けるが、堆積して地下深部に埋没する過程では、地下水との再平衡によって、未固結の泥質物質は続成作用によって固化し、安定な堆積岩となる。我々の生活において最も身近な粘土鉱物はスメクタイトである。このスメクタイトは地下環境において、アルカリ溶液との反応があると、溶解してゼオライト化するため、スメクタイトを主成分とする岩石であるベントナイトには必ずゼオライトが共存している。この現象を実験室で再現し、反応に必要な溶液や温度圧力条件を知ることは、未固結の粘土質物質が安定化する時間スケールを知る上で重要である。そこで、Naモンモリロナイトを1.0M NaOH溶液中120 °Cにて変質させ、ゼオライトの成長を位相シフト干渉計を使ってその場観察[1]した。単純化した反応式を表すと、 $3\text{Al}_2\text{Si}_4\text{O}_{10}(\text{OH})_2 + 2\text{NaOH} = 2\text{NaAlSi}_2\text{O}_6(\text{H}_2\text{O})$ である。この条件では、Naモンモリロナイトの溶解は $9.5\text{E}-10 \text{ mol/m}^2/\text{s}$ で進行し[2]、モル体積 $136.4\text{E}-6 \text{ m}^3/\text{mol}$ から求めた面溶解速度では $6.9\text{E}-6 \text{ m/s}$ となる。生成したアナルサイムの成長速度は $1.1\text{E}-10 \text{ m/s}$ であった。モンモリロナイトの溶解は反応表面積の増減で2-3桁変化できるが、それを考慮すると、溶解と成長の物質的バランスには大きな矛盾はない。しかし、反応前後の体積変化は $193.96 - 173.91 = +20.05 \text{ cm}^3/\text{mont mol}$ となり、この反応は体積拘束のある閉鎖系では抑制されることを意味している。さらに、シリンジ型セルを用いた大過剰のNaOHのある系での圧縮実験を行うと、ハイドロソーダライトが、 $3\text{Al}_2\text{Si}_4\text{O}_{10}(\text{OH})_2 + 20\text{NaOH} = \text{Na}_8\text{Al}_6\text{Si}_6\text{O}_{24}(\text{OH})_2 + 6\text{Na}_2\text{SiO}_3 + 12\text{H}_2\text{O}$ によって生成した。この反応前後の体積変化は $+54.67 \text{ cm}^3/\text{mont mol}$ であり、変質はさらに抑制される。このように反応系のアルカリは、粘土のゼオライト化反応を起こすが完全な置換には至らず、粘土の空隙を充填することで安定化することがわかる。

[1] Satoh et al. (2007) American Mineralogist, 92, 503-509.

[2] Sato et al. (2005) Proc. of the Int. Workshop on Bentonite-Cement Interaction in Repository Environments, A3-38-41.

キーワード：スメクタイト、ゼオライト化、成長速度、体積変化

Keywords: smectite, zeolitization, growth rate, volume change